

## Medical Image Segmentation with Improved Gradient Vector Flow

Jinyong Cheng, Xiaoyun Sun

School of Information, Shandong Provincial Key Laboratory of Fine Chemicals,  
Shandong Polytechnic University, Jinan, 250353 China

**Abstract:** In this study, we discover some deficiencies of GVF and GGVF Snake such as it can not capture boundaries like “U” and “Ω” completely because of the counteraction of some external forces and the influence of the local minimum external forces. Based on analyzing force distribution rules of gradient vector flow, a standard is introduced to distinguish every control point is true or false. An additional control force is added to GVF Snake model. The direction of control force is gained by tracking the force field and the motion of snake control points. Experimentation proves that the new GVF Snake model can solve the problem that GVF and GGVF Snake model can not detect the boundaries like “U” and “Ω” and the new algorithm can improve GVF snake model’s ability to capture thin boundary indentation like the boundary of brain image.

**Keywords:** Active contour models, edge detection, gradient vector flow, medical image segmentation

### INTRODUCTION

Image segmentation is an important issue in image processing, computer vision and pattern recognition, etc. In medical image processing, it is especially significant to get the boundary of the apparatus. Amongst a variety of image segmentation methods, the Gradient Vector Flow (GVF) technique by Xu and Prince (1998a, b) recently gains a wide attention due to its excellent performance to deal with concave regions (Xu and Prince, 1998a, b). The GVF snake uses a spatial diffusion of the gradient of an edge map, which replaces image gradients as an external force. Traditional snake is inherently weak in two main aspects: First, the initial border must be fairly close to the true boundary. Second active contours can not automatically converge to boundary concavities (Kass *et al.*, 1988). GVF Snake has a much larger capture range than traditional snake and can solve the main problems. And GVF snake have been widely used in image segmentation (Tang, 2009; Zhu *et al.*, 2010). However, some problems is discovered in this study that the GVF snake can not capture right object contours like “U” and “Ω” in some image. In the process of the snake approach the object contour, the control points move to the place at the image which the external force is lesser. it is not all the pixels with local minimum force are in true boundary of image. Because of this reason this snake fails to converge to the true boundary.

In this study, analysis of force field and experiments prove that the results of GVF snake model are related to the geometry of indentation when the snake approaches to concave boundaries. Specifically, when the pixels number of a long and thin boundary indentation is even, GVF snake can not capture the indentation and when the

number is odd number, GVF snake can capture the indentation. When the concave boundary is like a “Ω” shape, GVF snake can not capture the correct boundary. The major cause for this problem is that not all the pixels with local minimum force are true boundary points. We can see the boundary with a “Ω” shape as a bottle. At the bottle-neck, there is an area that the external force gets local minimum value. The snake stops and can not continue the approach to the true boundary. To solve these issues, based on analyzing force distribution rules of gradient vector flow, a standard is introduced to distinguish the false one from contour points. The result is not considered as final solution when the snake energy is minimal. Moreover the estimation and calculation should be done according to the established standard and then the result can be considered as the final one, so the snake is prevented from running into local minimum. An additional control force is added to GVF Snake model. The direction of control force is gained by tracking the force field and the motion of snake’s control points. Experimentation proves that the new GVF Snake model can solve the problem that GVF Snake model can not detect the boundaries like “U” and “Ω” and the new algorithm can improve GVF snake model’s ability to capture thin boundary indentation like the boundary of brain image.

### GVF AND GGVF ALGORITHM

**Basic theory of GVF snake:** Active contours, or snakes, have been widely studied and applied in image analysis. Their applications include edge detection (Kass *et al.*, 1988), segmentation of objects (Terzopoulos and Fleischer, 1988), shape modeling (Leymarie and Levine,

1993) and motion tracking (Terzopoulos and Szeliski, 1992). The snake presented by Kass *et al.* (1988) is an elastic curve, which from an initial state tries to change to the most appropriate state of the scene (Kass *et al.*, 1988). It is deformed due to external forces that attract it towards salient features of the image and internal forces which try to preserve the condition of smoothness in the shape of the curve. A final solution is given by the minimum total energy of the snake, which is the result of the equation:

$$E = \int_0^1 \left( \frac{1}{2} (\alpha |X'(s)|^2 + \beta |X''(s)|^2) + E_{ext}(X(s)) \right) ds \quad (1)$$

where  $\alpha$  and  $\beta$  are weighting parameters which control the snake's tension and rigidity, respectively,  $X'(s)$  and  $X''(s)$  denote the first and second derivatives of  $X(s)$  with respect to  $s$ . The external energy function  $E_{ext}$  is derived from the image so that it takes on its smaller values at the features of interest, such as boundaries.

Given a gray level image  $I(x, y)$  which viewed as a function of continuous position variables  $(x, y)$ , typical external energies designed to lead an active contour toward step edges are:

$$E_{ext}^1(x, y) = -|\nabla I(x, y)|^2 \quad (2)$$

$$E_{ext}^2(x, y) = -|\nabla (G_\sigma(x, y) * I(x, y))|^2 \quad (3)$$

where  $G_\sigma(x, y)$  is a two-dimensional Gaussian function with standard deviation  $\sigma$  and  $\nabla$  is the gradient operator. A snake that minimizes  $E$  must satisfy the Euler equation:

$$\alpha X^{(2)}(s) - \beta X^{(4)}(s) - \nabla E_{ext} = 0 \quad (4)$$

To find a solution to (4), the snake is made dynamic by treating  $X$  as function of time  $t$  as well as  $s$  which i.e.  $X(s, t)$ . Then, the partial derivative of  $X$  with respect to  $t$  is then set equal to the left hand side of (4) as follows:

$$X_t(s, t) = \alpha X^{(2)}(s) - \beta X^{(4)}(s) - \nabla E_{ext} \quad (5)$$

When the solution  $X(s, t)$  stabilizes, the term  $X_t(s, t)$  vanishes and we achieve a solution of (4). This dynamic equation can also be viewed as a gradient descent algorithm designed to solve (1). A solution to (5) can be found by discretizing the equation and solving the discrete system iteratively.

Although the traditional snake has found many applications, it is intrinsically weak in two main aspects: First, the initial border must be fairly close to the true boundary. Second active contours do not necessarily converge to boundary concavities. An example of traditional snake applied to a medical image is shown in Fig. 1. Figure 1a shows a medical image with knob and an

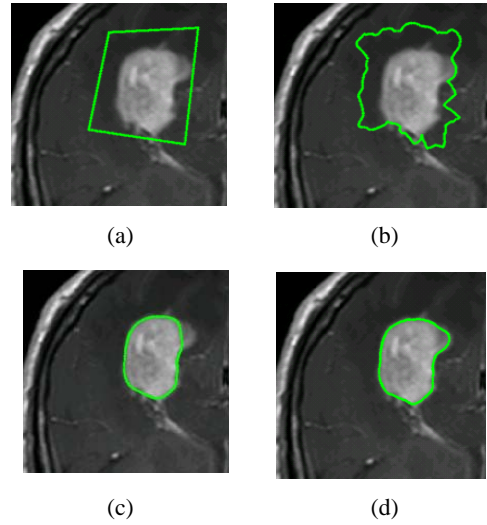


Fig. 1: (a) Initial border, (b) convergence using a traditional snake, (c) convergence using a GVF snake,  $\alpha = 2$ , (d) convergence using a GVF snake,  $\alpha = 0.5$

initial border. Figure 1b shows the border output of snake. Figure 1c and d shows the border output of GVF snake. Because the initial border is far from the true boundary, the active contours can not converge to the true boundary. Clearly, the capture range of traditional snake is very small. To GVF Snake with  $\beta = 0$ , when  $\alpha = 2$ , part of object boundary is lose. And when  $\alpha = 0.5$  the boundary is appropriate and full.

To solve the issue of traditional snake, Cohen (1991) has imported external force to expand and shrink the active contour (Cohen, 1991), but it is not easy to ensure the force. Williams and Shah (1991) have presented fast greedy algorithm to carry out the snake model and this method reduced the time cost (Williams and Shah, 1991). Eviatar and Soorjai (1996) have presented an algorithm to solve the problem about the boundary concavities (Eviatar and Soorjai, 1996), but the initialization of original snake need manual work. Xu and Prince (1998a, b) have proposed a new deformable model called Gradient Vector Flow (GVF) snake (Xu and Prince, 1998a, b). The GVF snake model remedied both of the shortcomings of the traditional snake. The basic idea of the GVF snake is to extend influence range of image force to a larger area by generating a GVF field. The GVF field is computed from the image. In detail, a GVF field is defined as a vector field  $V(x, y) = (u(x, y), v(x, y))$  that minimizes the energy function:

$$E = \iint \mu (u_x^2 + u_y^2 + v_x^2 + v_y^2) + |\nabla f|^2 |V - f|^2 dx dy \quad (6)$$

where,  $f$  is the edge map which is derived by using an edge detector on the original image convoluted with a

Gaussian kernel and  $\mu$  is a regularization parameter. When  $|\nabla f|$  is small, the energy is dominated by the sum of the squares of the partial derivatives of the vector field, resulting a slowly varying yet large coverage field. On the other hand, when  $|\nabla f|$  is large, the second term dominates the integral.

Using the calculus of variations, the GVF field can be obtained by solving the following Euler-Lagrange equations:

$$\mu \nabla^2 u - (u - f_x)(f_x^2 + f_y^2) = 0 \tag{7}$$

$$\mu \nabla^2 v - (v - f_y)(f_x^2 + f_y^2) = 0 \tag{8}$$

where,  $\nabla^2$  is the Laplacian operator.

**Limitation of GVF snake:** Comparing the result in Fig. 1d to the traditional snake result in Fig. 1b, we can see that most of the active contours converge to the true boundary. The GVF snake has a much larger capture range than traditional snake. But the GVF snake can not capture right object contours in some image. In the process of the snake approach the object contour, the control points move to the place at the image which the external force is lesser. However, it is not all the pixels with local minimum force are in true boundary of image. Because of this reason this snake fails to converge to the true boundary. To deal with these problems we have developed an improved GVF snake. This new method is presented in detail in the following section.

When the concave boundary is like a “ $\Omega$ ” shape, GVF snake can not capture the correct boundary. The major cause for this problem is that not all pixels with local minimum force are true boundary points. We can see the boundary with a “ $\Omega$ ” shape as a bottle. At the bottle-neck, there is an area that the external force gets local minimum value. The snake stops here and can not continue the approach to the true boundary.

Figure 2 shows the result of GVF snake applied to a “ $\Omega$ ” shape boundary with  $\alpha = 0.5$ ,  $\beta = 0$ . From the result of the experiment we can see that the GVF snake can not capture “ $\Omega$ ” shape boundary.

Based on the Euler-Lagrange Eq. (7) and (8), we have the iterative formula to get the GVF force field:

$$u = u + \mu \nabla^2 u - (u - f_x)(f_x^2 + f_y^2) \tag{9}$$

$$v = v + \mu \nabla^2 v - (v - f_y)(f_x^2 + f_y^2) \tag{10}$$

Under the operation of Laplacian operator  $\nabla^2$  and iterative formula (9) and (10), the external force diffuses from pixels with big gradient to pixels with small

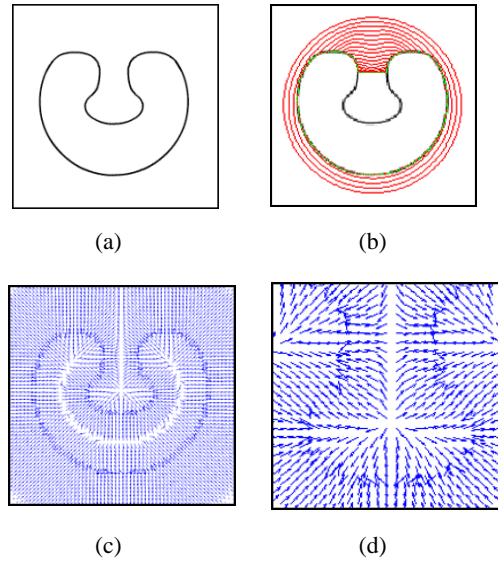


Fig. 2: (a) An image with a “ $\Omega$ ” boundary, (b) convergence of GVF snake, (c) force field of GVF snake, (d) local force field of GVF snake

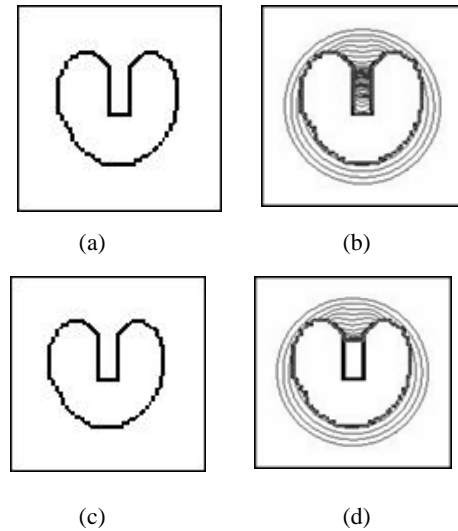


Fig. 3: (a), (b) Convergence to indentation with 7 pixels, (c), (d) convergence to indentation with 8 pixels

gradient. In the process, some external forces are counteracted each other.

Figure 3 shows the result of GVF snake applied to four images with thin boundary indentation with  $\alpha = 0.5$ ,  $\beta = 0$ . The interval of the indentation in Fig. 3a is 7 white pixels. Figure 3c is 8. Figure 3b, d are convergence result of GVF snake to the thin boundary indentation. We can see that when the pixels number of the indentation is even, GVF snake can not capture the indentation and when the pixels number of the indentation is odd number, GVF snake can capture the indentation. The external force

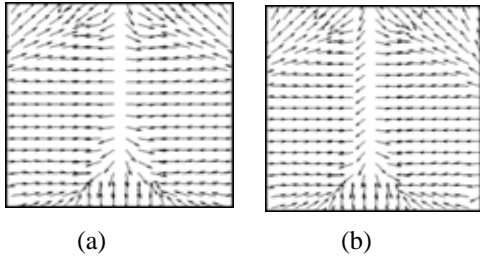


Fig. 4: (a) GVF force field with even number interval, (b) GVF force field with odd number interval

field images are shown in Fig. 4. Figure 4a is GVF force field with even interval and Fig. 4b is GVF force field with odd number interval. It is clear that when the pixels number of the indentation is even, the force in vertical direction is counteracted by the force in horizontal direction. And when the pixels number of the indentation is odd number, the force in vertical direction still exists.

To improve active contour convergence into long, thin boundary indentations, Xu and Prince (1998a, b) presented GGVF snake model. It is a generalization of GVF formulation includes two spatially varying weighting functions. The GGVF is defined as the following vector partial differential equation:

$$v_t = g(|\nabla f|)\nabla^2 v - h(|\nabla f|)(v - \nabla f) \quad (11)$$

The first term on the right is referred to as the smoothing term because this term can produce a smoothly varying vector field. The second term is referred as the data term since it encourages the vector field  $v$  to be close to  $\nabla f$ . The weighting functions  $g(\cdot)$  and  $h(\cdot)$  apply to the smoothing and data terms, respectively.

The above equation reduces to be GVF when:

$$g(|\nabla f|) = \mu \quad (12)$$

$$h(|\nabla f|) = |\nabla f|^2 \quad (13)$$

Since  $g(\cdot)$  is constant here, smoothing occurs everywhere; however,  $h(\cdot)$  grows larger near strong edges and should dominate at the boundaries. There are many ways to specify such pairs of weighting functions. Here we use the following weighting functions for GGVF:

$$g(|\nabla f|) = e^{-\left(\frac{|\nabla f|}{k}\right)^2} \quad (14)$$

$$h(|\nabla f|) = 1 - g(|\nabla f|) \quad (15)$$

The contour results of the GVF snake and GGVF snake to long, thin boundary are shown in Fig. 5 with  $\alpha = 0.5$ ,  $\beta = 0$ . It can be found that while the pixels

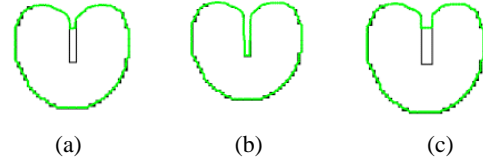


Fig. 5: (a) Result of GVF snake with 5 pixels interval, (b) result of GGVF snake with 5 pixels interval, (c) result of GGVF snake with 8 pixels interval

number of the indentation is 5, the interval is so thin that the GVF snake can't approach the object boundary. But the GGVF can obtain true boundary. While the pixels number of the indentation is even number, the GGVF can obtain true boundary too. The reason is that in the process of the external force diffuses from pixels with big gradient to pixels with small gradient, some external forces are counteracted each other.

**Improved algorithm:** We put forward an improved algorithm by tracking the original GVF force and adding a new external force to solve the above problems. The force balance equation of GVF snake model is:

$$F_{int} + F_{ext} = 0 \quad (16)$$

where,  $F_{int}$  and  $F_{ext}$  are expressed by Eq. (6). In this study, a new external force  $F_{ext2}$  is presented and the force balance equation of new snake model is:

$$F_{int} + F_{ext1} + F_{ext2} = 0 \quad (17)$$

where,  $F_{ext1}$  corresponds with  $F_{ext}$  in Eq. (16). The additional force  $F_{ext2}$  is adaptive and it can confirm its size and direction timely to improve the performance of snake based on the position and force field of the control points. When the GVF snake energy is minimal, the result is not considered as final result. The estimation and calculation should be given according to the established standard. If the GVF snake is not final result after the estimation, the additional force  $F_{ext2}$  will work and will force the snake to the true boundary. And then the result can be considered as the final one. Or else the GVF snake result is the final result and the size of  $F_{ext2}$  is zero. That is to say, whether the additional force  $F_{ext2}$  will work is decided by the established standard and the force field of the control points.

Based on the above ideas and the GVF force field, the steps of the improved algorithm are as follows:

- Select an appropriate preprocessing method to process the primary image according to the characteristics of the primary image. And a preprocessed image is obtained. The general image preprocessing methods include Gaussian smoothing, wavelet transform (Mallat and Hwang, 1992) and

image binaryzation, etc. Calculate GVF force field of the preprocessed image based on Eq. (6). The external force of the improved algorithm is composed of  $F_{ext1}$  and  $F_{ext2}$  in Eq. (17). The GVF force is  $F_{ext1}$  and the value of  $F_{ext2}$  is zero at this time. Initialize the snake in the external force field and deform it until the contour can not be changed, then an interim result is obtained. The energy of the interim result is a local minimum or a global minimum.

- Analysis every contour point of the interim result and judge whether the point is true contour point or false contour point. The existence of false contour points is the reason why the energy of the snake can not approach the global minimum. If there are continuous false contour points in the interim result of the snake, we should change the external force field in a specific area. The specified area is between the continuous false contour points and the corresponding true contour points. After the calculation of the new external force field, deform the snake until the places of the contour points is steady. Then, a new interim result is obtained. Judge every contour point of the new interim result is true or false contour point. Repeat this process and if there are no false contour points in the interim result, the algorithm is finished.

In order to perform the idea, two problems should be resolved. First, how to decide whether the GVF snake is final result? Second, while the GVF snake is not final result, how to find the true boundary using the additional force  $F_{ext2}$ ?

The determination of true contour points and false contour points is given here. Six sorts of true contour points of distance potential force field and FFA snake are introduced by Hou and Han (2005). The six sorts of true contour points are normal contour point, 16-pair contour point, broken point, center contour point, zero point, special contour point, false contour point and its corresponding contour point, post-update contour. In FFA snake, all points in the curve must be judged to be one of the six sorts of the true contour points when the energy of the snake is approaching the minimum. This study proposes a practical and simple method to judge true and false contour points based on GVF force field.

An interim result is obtained after a snake deforming in the GVF force field. To every point of the interim curve, find relative position of the contour point in the original image and calculate the gradient value of the image region. If the original image has big noise, the image region for calculating gradient can range eight neighborhoods or sixteen neighborhoods. The curve point can be seen as true contour point if the gradient value is more than a specified threshold which marked as  $T_1$ . If the gradient value of an image region is smaller than

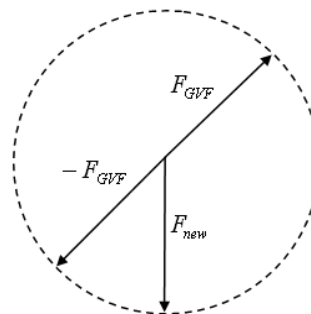


Fig. 6: The idea of new external force model

threshold  $T_1$ , the curve point in the image region can not be judged as a true point. To avoid the disturbances of short interval in the boundary line, we should analysis the number of these curve points which being linked together. If the number of the curve points which being linked together and having low gradient is small, these curve points should be judged as true contour points. When the length of these continuous points is more than the specified length threshold, these curve points can be seen as false contour points temporarily. Here, the length threshold value is set to 3. And under the influence of external force  $F_{ext2}$ , the corresponding contour points should be found. If the corresponding contour points are found, these curve points should be judged as false contour points and the GVF force field should be changed by  $F_{ext2}$ . If the corresponding contour points are not found, the GVF force field should not be changed and these contour points should be seen as true contour points.

How to use the additional force  $F_{ext2}$  to find the true boundary while the GVF snake is not final result? At first, determine whether there are continuous points which have small gradient based on the above definition. Select two ends of the continuous contour points and connect the two points as a line. There are two vertical directions of the line. One vertical direction is where the snake comes from and the other vertical direction is the direction of the additional force  $F_{ext2}$ . The angle between abscissa and the direction of the additional force  $F_{ext2}$  is set to  $\theta$ . After the additional force  $F_{ext2}$  is added, the final force is marked as  $F_{new}$ . Here, the computational method of final force is not only one. So long as the new force can guide the snake to overcome the obstacles region, the computational method should be practicable. For example, as shown in Fig. 6, the angle value of  $F_{new}$  is set to  $\theta$ . Original GVF force is marked as  $F_{GVF}$ . And  $F_{GVF}$  is equal to  $F_{ext1}$ . The calculating formula is:

$$F_{ext2} = F_{ext1} - F_{GVF} + F_{new} \tag{18}$$

The magnitude of  $F_{new}$  and  $F_{GVF}$  is equal:

$$|F_{new}| = |F_{GVF}| \tag{19}$$

The direction of  $F_{new}$  is same with the direction of the additional force:

$$A(F_{new}) = \theta \quad (20)$$

These formulas can guarantee that the direction of the final resultant force is the vertical direction to the line composed of the false contour points. The magnitude of the final resultant force is equal to the force of original GVF. To improve the computation speed, another simple method is that set the magnitude of the final resultant force to the maximum value of all the original GVF force of every pixel.

The size of the force  $F_{ext2}$  can be set as the biggest one of all the values of original GVF force. Along the search direction, each search step will reach a point. Judge the gradient value of this point and if the gradient value is smaller than a specific threshold which marked as  $T_2$ , apply external force  $F_{ext2}$  to this point and reach the next point in the search direction. The influence of the external force  $F_{ext2}$  will continue until find a point and the gradient value of the point is more than the threshold. Then an improved GVF force field is obtained and the interim GVF snake can continue to approach under the new force field.

When judging whether a control point is true or false control point, a specified gradient threshold is marked as  $T_1$ . When judging whether the new snake should stop approaching, another specified gradient threshold is marked as  $T_2$ . In fact,  $T_2$  is used to judge if the snake reach true edge point. So, we can set the two thresholds  $T_1$  and  $T_2$  to be a equal value.

### EXPERIMENTAL RESULTS

This section shows several examples obtained by using improved algorithm on simple objects and real medical images. The result of simulation experiments confirm the feasibility and correctness of the improved algorithm to detect the boundaries like “U” and “Ω”.

The first experiment shows the new external force field for the same U-shaped object used in Fig. 2c. Figure 7 shows the new experimental result with  $\alpha = 0.5$ ,  $\beta = 0$ . Figure 7a shows output and Fig. 7b shows the new external force field. We can see that the new algorithm can avoid the disturbance of the force in horizontal direction.

Figure 8 shows the result of improved algorithm applied to Fig. 2a with  $\alpha = 0.5$ ,  $\beta = 0$ . From these experiments we can see that the improved algorithm can solve the problem that GVF Snake model can not detect the boundaries like U and bottleneck and the new algorithm can improve GVF snake model’s ability to capture thin boundary indentation.

Figure 9 shows the result of improved algorithm applied to a real human brain image with  $\alpha = 0.5$ ,  $\beta = 0$ . Because the middle part of the brain image is blurred,

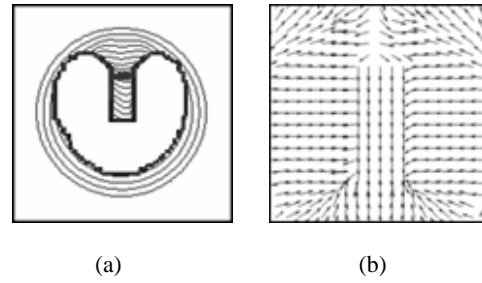


Fig. 7: (a) Convergence with improved algorithm , (b) improved external force field

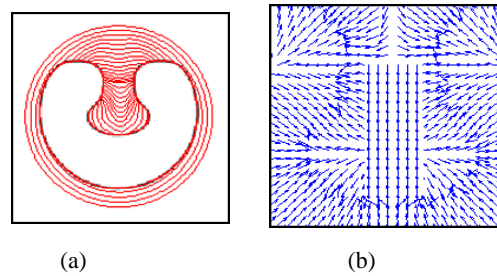


Fig. 8: (a) Convergence with improved algorithm (b) improved external force field

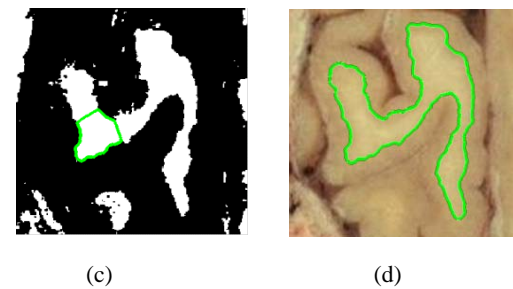
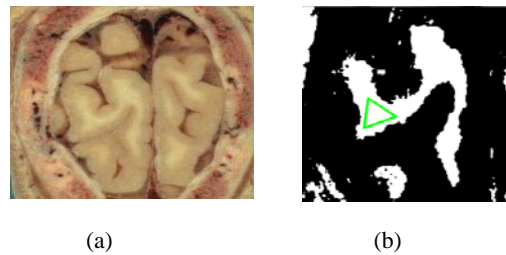


Fig. 9: (a) A human brain image, (b) initial border, (c) convergence using a GVF snake, (d) convergence with improved algorithm

preprocessing to original image is essential before the snake model is used. There are several usual image preprocessing methods such as Gaussian smoothing, wavelet transform and image binarization. In this image, the color of object area is similar. So we can perform image binarizing process to the image. Then GVF snake model is used to approach the object boundary. As shown

in Fig. 9c, this GVF snake fails to converge to the true boundary. In Fig. 9d, further treatment to false contour point of the snake by the improved algorithm in this study, true object boundary can be obtained. Clearly, the improved GVF snake has a broad capture range and superior convergence properties.

### CONCLUSION

An improved GVF snake model is presented in this study which can detect thin boundaries and “ $\Omega$ ” shape boundaries. Because some external forces cancel out each other, the performances of GVF snake model are related to the geometry of indentation while long and thin boundaries are approached. When a concave boundary is like a “ $\Omega$ ” shape, GVF snake can not capture the correct boundary too. To solve the problems, a standard is put forward to distinguish the true and false contour points. While the original GVF snake stops approaching, an additional external force is added to the false control points. The direction of the control force is determined by tracking the force field and the motion of the snake's control points. Experiments indicate that the new algorithm can improve GVF snake model ability to capture the thin boundary indentation. On the side, the improved method proposed in this study can be applied to converge bottleneck shape image and medical image.

The model algorithm and computer program is an improvement over the existing GVF snake model. However the standard of this study is still based on the calculation of gradient vector when judging if the new snake has a correct convergence. So, the accuracy of the new algorithm is guaranteed. Since it needs to judge true or false contour points and calculate the external force, the time for computer to complete the new algorithm is slightly higher than original GVF snake. In practical application the positive rate of false contour points is smaller than true contour. Therefore the gap of efficiency is not much.

### ACKNOWLEDGMENT

This study is supported by A Project of Shandong Province Higher Educational Science and Technology

Program (J10LG20), China and by Natural Science Foundation of Shandong Province (ZR2011FQ038), China.

### REFERENCES

- Cohen, L.D., 1991. Note: On active contour models and balloons. *CVGIP- Image understand.*, 53(2): 211-218.
- Eviatar, H. and R. Soorjai, 1996. A fast, simple active contour algorithm for biomedical images pattern. *Recogn. Lett.*, 55: 969-974.
- Hou, Z. and C. Han, 2005. Force field analysis snake: An improved parametric active contour model. *Pattern Recogn. Lett.*, 26: 513-526.
- Kass, M., A.P. Witkin and D. Terzopoulos, 1988. Snakes: Active contour models. *Int. J. Comput. Vis.*, 1(4): 321-331.
- Leymarie, F. and M.D. Levine, 1993. Tracking deformable objects in the plane using an active contour model. *IEEE T. Pattern Anal.*, 15: 617-634.
- Mallat, S. and W. Hwang, 1992. Singularity detection and processing with wavelets. *IEEE Trans. Inform. Theor.*, 38: 617-643.
- Tang, J., 2009. A multi-direction GVF snake for the segmentation of skin cancer images. *Pattern Recogn.*, 42: 1172-1179.
- Terzopoulos, D. and K. Fleischer, 1988. Deformable models. *Visual Comput.*, 4(6): 306-331.
- Terzopoulos, D. and R. Szeliski, 1992. Tracking with Kalman snakes. *Active Vision, Artificial Intelligence.* The MIT Press, Cambridge, Massachusetts, pp: 3-20.
- Williams, D.J. and M. Shah, 1991. A fast algorithm for active contours and curvature estimation. *CVGIP- Image understand.*, 55: 14-26.
- Xu, C. and J. Prince, 1998a. Snakes, shapes and gradient vector flow. *IEEE T. Images Proc.*, 7: 359-369.
- Xu, C. and J. Prince, 1998b. Generalized gradient vector flow external forces for active contours. *Signal Proc.*, 71: 131-139.
- Zhu, G., S. Zhang, Q. Zeng and C. Wang, 2010. Gradient vector flow active contours with prior directional information. *Pattern Recogn. Lett.*, 31(9): 845-856.